Supplementary Material (ESI) for Dalton Transactions

Supplementary Material

Lanthanide-3d Cyanometalate Chains Ln(III)-M(III) (Ln = Pr, Nd, Sm, Eu, Gd, Tb; M = Fe) with the Tridentate Ligand 2,4,6-tri(2-pyridyl)-1,3,5-triazine (tptz): Evidence of Ferromagnetic Interactions for the Sm(III)-M(III) compounds (M = Fe, Cr)

Hanhua Zhao, Nazario Lopez, Andrey Prosvirin, Helen T. Chifotides, and Kim R. Dunbar*

Figures S1-S13.

Tables S1-S5.

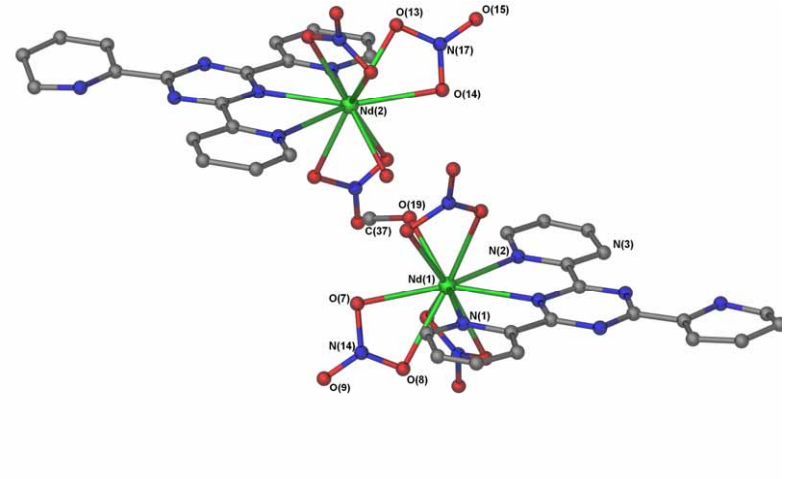

Figure S1. Structure of $[Nd(tptz)(NO_3)_3(H_2O)][Nd(tptz)(NO_3)_3(CH_3OH)]$.

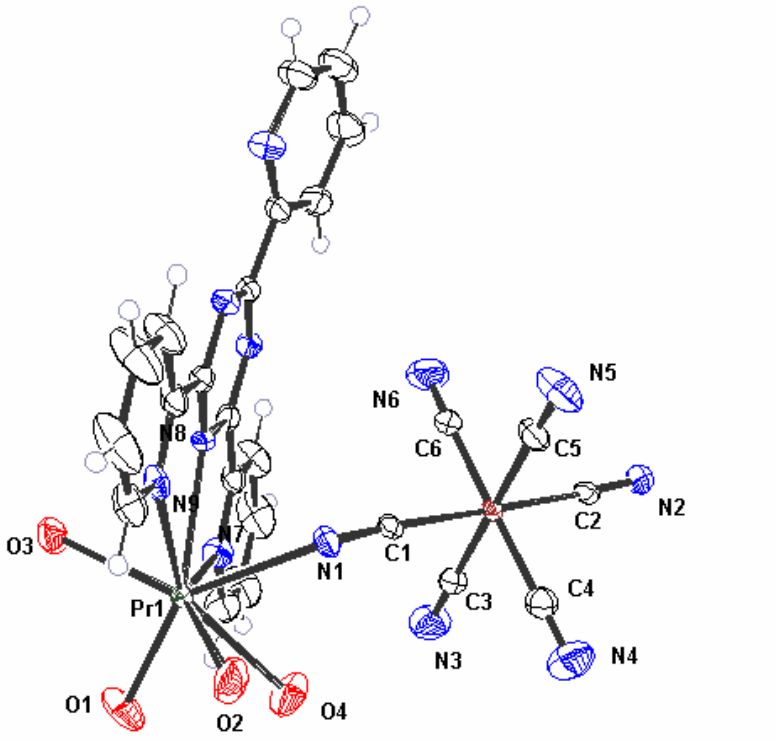

Figure S2. Thermal ellipsoid plot for $\{[Pr(tptz)(H_2O)_4Fe(CN)_6]\cdot 8H_2O\}_\infty$ (**1**) drawn at the 50% probability level; water crystallization molecules in the lattice have been omitted for the sake of clarity.

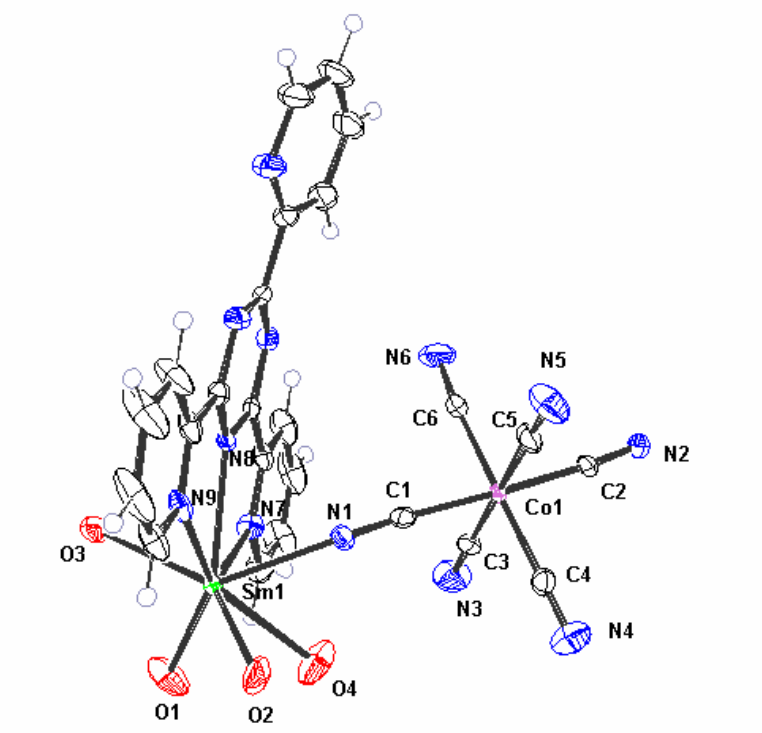

Figure S3. Thermal ellipsoid plot for $\{[Sm(tptz)(H_2O)_4Co(CN)_6]\cdot 8H_2O\}_\infty$ (**7**) drawn at the 50% probability level; water molecules of crystallization in the lattice have been omitted for the sake of clarity.

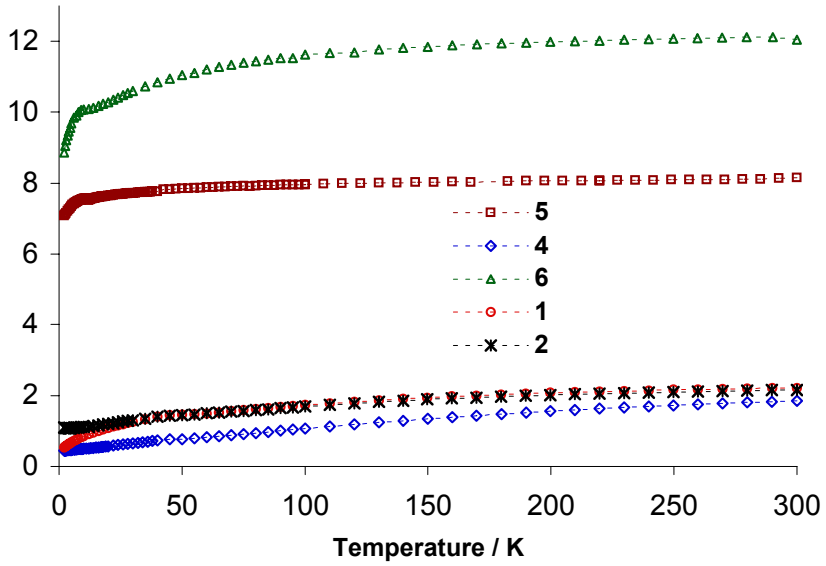

Figure S4. Temperature dependence of the χT product for compounds **1** (o), **2** (*), **4** (◊), **5** ( ), **6** (Δ).

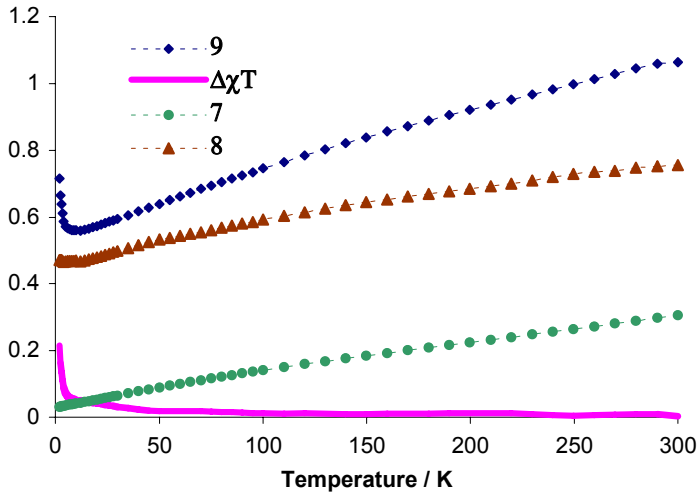

Figure S5. Temperature dependence of the χT product for compounds **9** (◊), **7** (o), **8** (Δ). The solid line represents the difference $\Delta\chi T = \chi T$ (**9**) - χT (**7**) - χT (**8**).

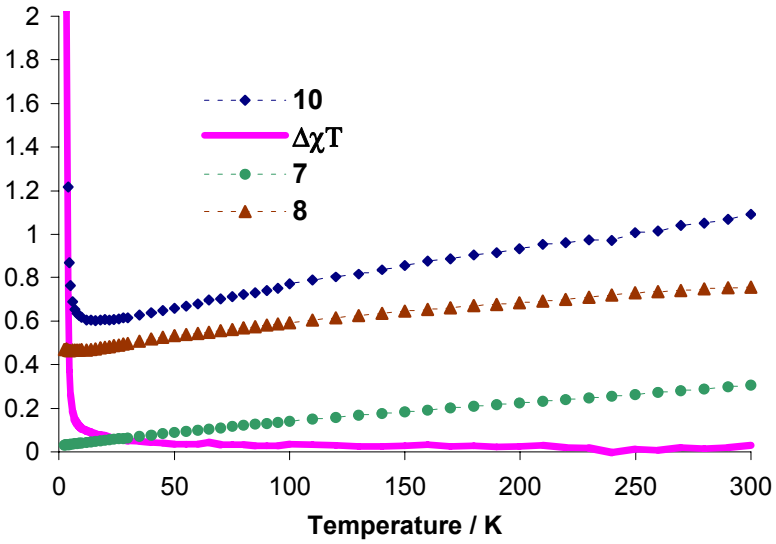

Figure S6. Temperature dependence of the χT product for compounds **10** (◊), **7** (o), **8** (Δ). The solid line represents the difference $\Delta\chi T = \chi T$ (**10**) - χT (**7**) - χT (**8**).

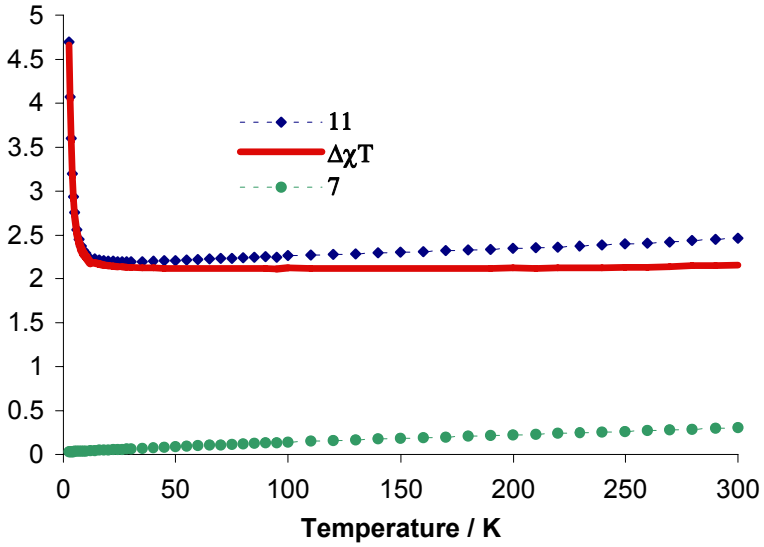

Figure S7. Temperature dependence of the χT product for compounds **11** (◊), **7** (o). The solid line represents the difference $\Delta\chi T = \chi T$ (**11**) - χT (**7**).

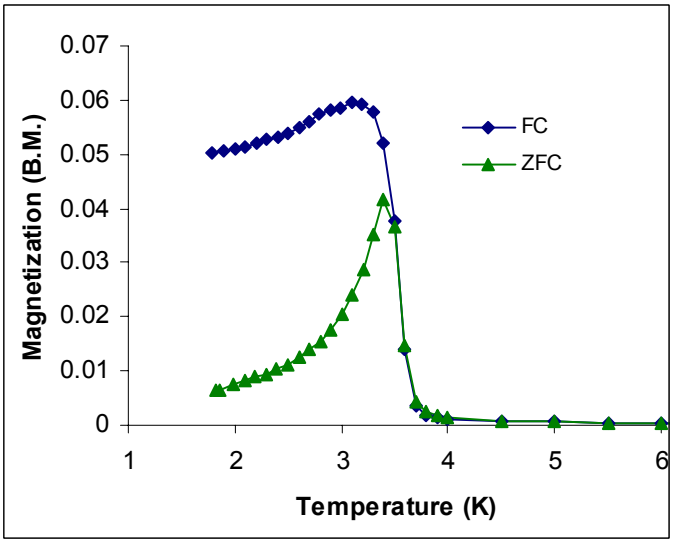

Figure S8. Temperature dependence of magnetization in the zero-field-cooling (ZFC) and field-cooling (FC) regime for **10** at magnetic field of 10 Oe.

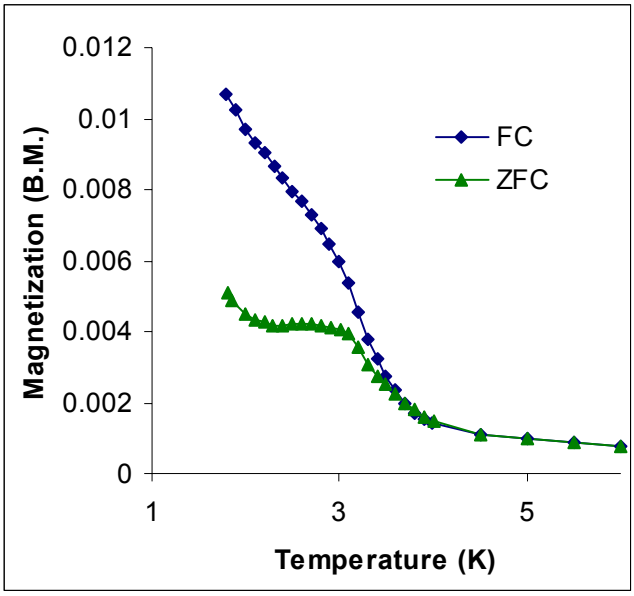

Figure S9. Temperature dependence of magnetization in the zero-field-cooling (ZFC) and field-cooling (FC) regime for **11** at magnetic field of 10 Oe.

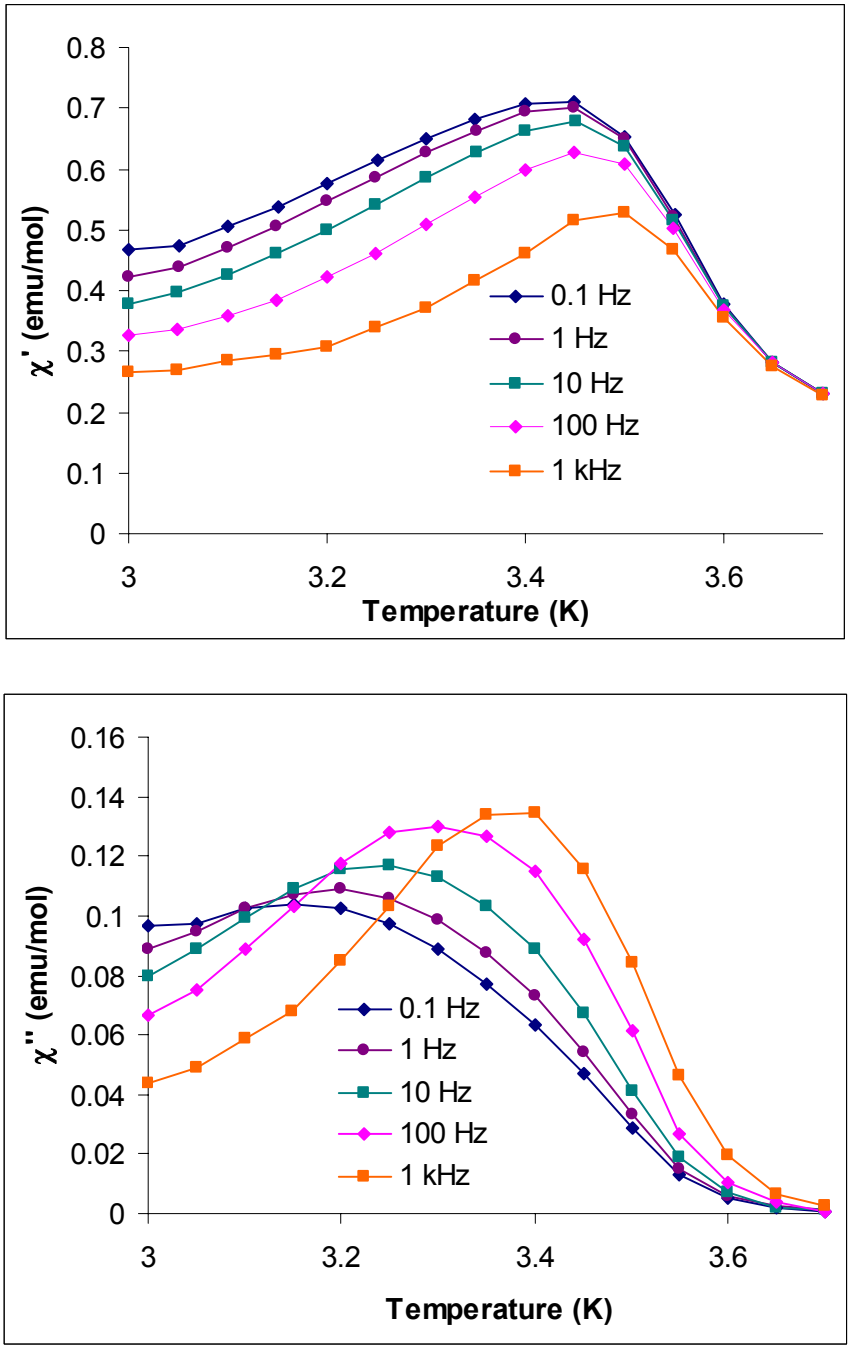

Figure S10. Temperature dependence of the real χ′ (top) and imaginary χ′′ (bottom) components of the ac susceptibility for **3** in vicinity of the phase transition.

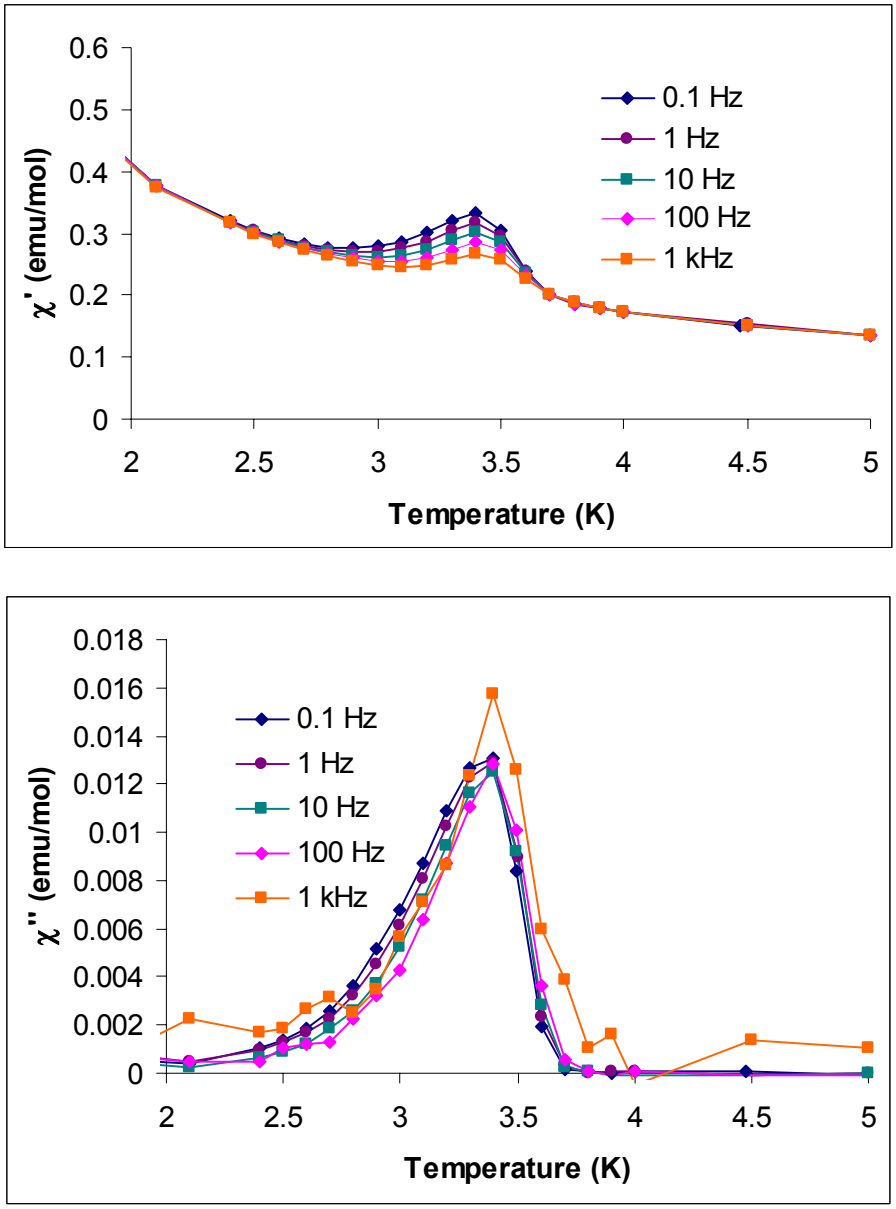

Figure S11. Temperature dependence of the real χ´ (top) and imaginary χ´´ (bottom) components of the ac susceptibility for **9**.

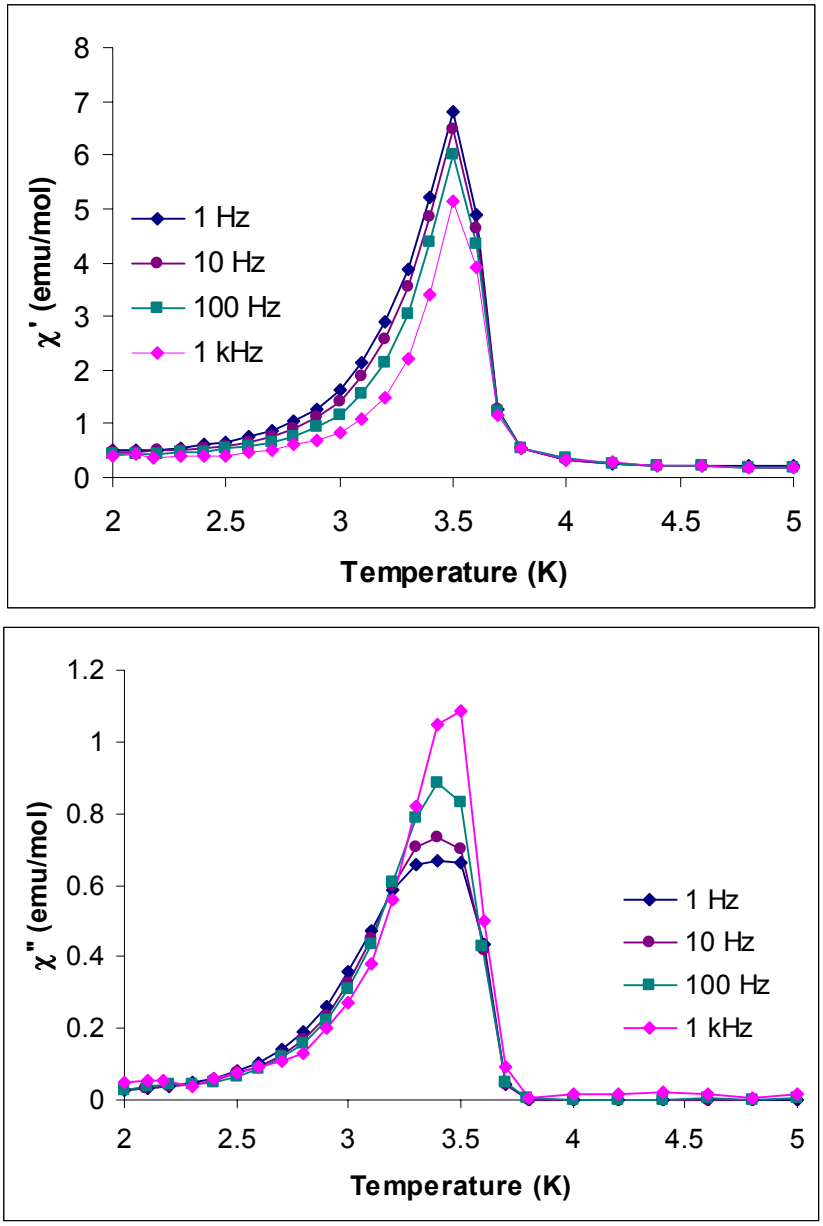

Figure S12. Temperature dependence of the real χ´ (top) and imaginary χ´´ (bottom) components of the ac susceptibility for **10**.

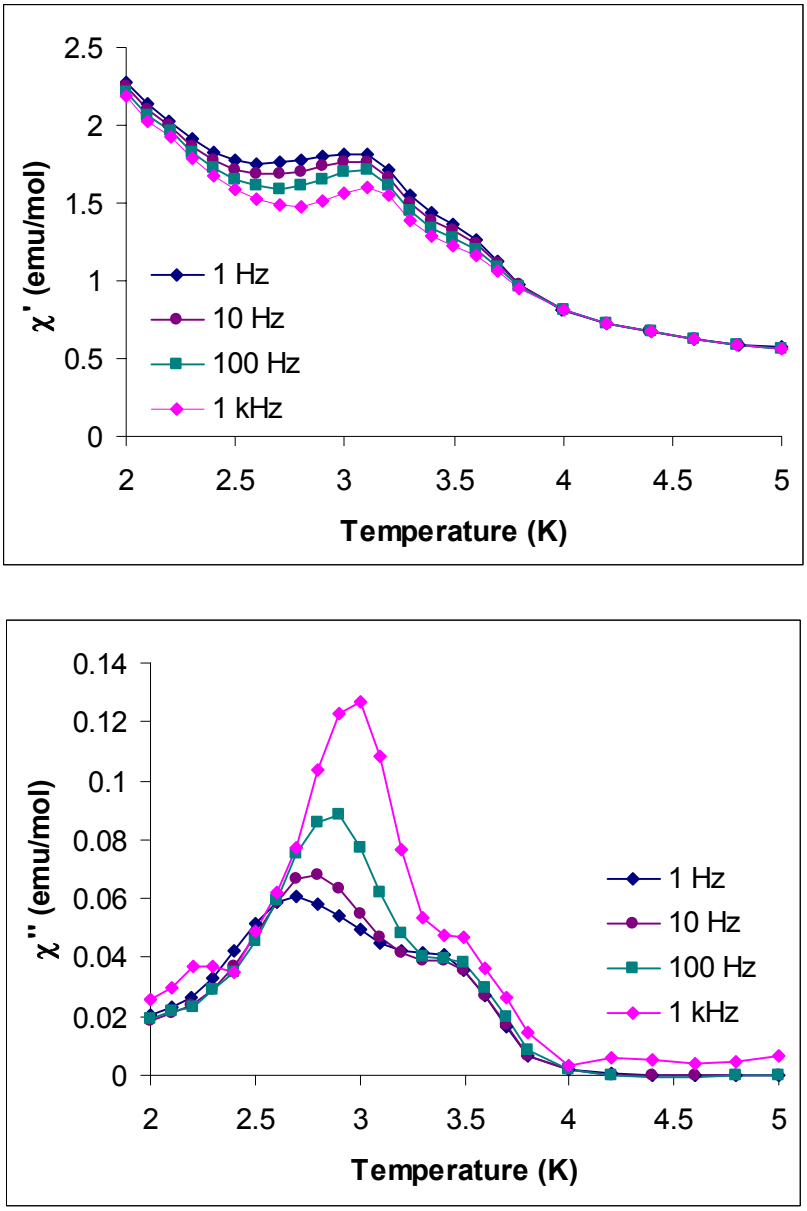

Figure S13. Temperature dependence of the real χ′ (top) and imaginary χ′′ (bottom) components of the ac susceptibility for **11**.

Table S1. Selected bond lengths (Å) and angles (º) for compound **1**.

Pr1-O(1)	2.492(5)	Fe(1)-C(3)	1.935(6)
Pr1-O(2)	2.484(5)	Fe(1)-C(4)	1.938(7)
Pr1-O(3)	2.512(4)	Fe(1)-C(5)	1.941(6)
Pr1-O(4)	2.533(5)	Fe(1)-C(6)	1.939(7)
Pr(1)-N(1)	2.566(5)	C(1)-N(1)	1.151(7)
Pr(1)-N(2)	2.535(5)	C(2)-N(2)	1.151(7)
Pr(1)-N(7)	2.683(5)	C(3)-N(3)	1.143(8)
Pr(1)-N(8)	2.640(4)	C(4)-N(4)	1.144(9)
Fe(1)-C(1)	1.923(6)	C(5)-N(5)	1.142(8)
Fe(1)-C(2)	1.917(6)	C(6)-N(6)	1.154(9)
N1-Pr1-N2	135.37(18)	C1-Fe1-C2	177.1(3)
N1-Pr1-N7	84.68(16)	C1-Fe1-C3	87.6(2)
N1-Pr1-N8	65.99(15)	C1-Fe1-C4	90.3(3)
N1-Pr1-N9	75.09(15)	N1-C1-Fe1	174.8(5)
N2-Pr1-N7	139.80(17)	N2-C2-Fe1	176.0(5)
C1-N1-Pr1	147.1(4)	C2-N2-Pr1	169.9(5)

Table S2. Selected bond lengths (Å) and angles (º) for compound **3**.

Sm1-O(1)	2.453(5)	Fe(1)-C(3)	1.942(7)
Sm1-O(2)	2.428(5)	Fe(1)-C(4)	1.945(7)
Sm1-O(3)	2.454(5)	Fe(1)-C(5)	1.942(7)
Sm1-O(4)	2.503(6)	Fe(1)-C(6)	1.940(8)
Sm(1)-N(1)	2.519(5)	C(1)-N(1)	1.148(8)
Sm(1)-N(2)	2.501(5)	C(2)-N(2)	1.142(8)
Sm(1)-N(7)	2.637(6)	C(3)-N(3)	1.144(9)
Sm(1)-N(8)	2.587(5)	C(4)-N(4)	1.147(9)
Fe(1)-C(1)	1.929(6)	C(5)-N(5)	1.141(9)
Fe(1)-C(2)	1.921(7)	C(6)-N(6)	1.157(10)
N1-Sm1-N2	135.61(19)	C1-Fe1-C2	177.1(3)
N1-Sm1-N7	84.60(18)	C1-Fe1-C3	87.9(2)
N1-Sm1-N8	66.17(18)	C1-Fe1-C4	90.1(3)
N1-Sm1-N9	75.79(17)	N1-C1-Fe1	173.9(5)
N2-Sm1-N7	139.74(19)	N2-C2-Fe1	175.9(6)
C1-N1-Sm1	148.1(5)	C2-N2-Sm1	169.6(5)

Table S3. Selected bond lengths (Å) and angles (º) for compound **7**.

Sm1-O(3)	2.461(5)	Co(1)-C(5)	1.889(7)
Sm1-O(4)	2.498(6)	Co(1)-C(6)	1.896(7)
Sm(1)-N(1)	2.517(5)	C(1)-N(1)	1.157(8)
Sm(1)-N(2)	2.496(6)	C(2)-N(2)	1.150(8)
Sm(1)-N(7)	2.627(6)	C(3)-N(3)	1.143(8)
Sm(1)-N(8)	2.580(5)	C(4)-N(4)	1.146(9)
Co(1)-C(1)	1.882(6)	C(5)-N(5)	1.149(9)
Co(1)-C(2)	1.881(6)	C(6)-N(6)	1.148(9)
N1-Sm1-N2	136.37(19)	C1-Co1-C2	176.8(3)
N1-Sm1-N7	84.04(17)	C1-Co1-C3	88.1(3)
N1-Sm1-N8	66.48(16)	C1-Co1-C4	91.1(3)
N1-Sm1-N9	76.33(16)	N1-C1-Co1	174.6(5)
N2-Sm1-N7	139.56(18)	N2-C2-Co1	175.4(6)
C1-N1-Sm1	148.3(5)	C2-N2-Sm1	170.3(5)

Table S4. Selected bond lengths (Å) and angles (º) for compound **10**.

Sm(1)-N(1)	2.457(5)	Fe(1)-C(4)	1.938(6)
Sm(1)-N(2)	2.456(5)	Fe(2)-C(2)	1.907(6)
Sm(1)-N(7)	2.573(4)	C(1)-N(1)	1.158(7)
Sm(1)-N(8)	2.579(4)	C(2)-N(2)	1.154(7)
Fe(1)-C(1)	1.906(6)	C(3)-N(3)	1.159(7)
Fe(1)-C(3)	1.948(6)	C(4)-N(4)	1.162(7)
N1-Sm1-N2	145.04(15)	N2-C2-Fe2	177,6(5)
N1-Sm1-O1	76.14(15)	C1-Fe1-C3	88.3(2)
N1-Sm1-O2	72.44(15)	C1-Fe1-C4	89.7(2)
C1-N1-Sm1	164.5(4)	C3-Fe1-C4	88.9(2)
C2-N2-Sm1	168.8(4)	O1-Sm1-O2	83.77(13)
N1-C1-Fe1	176.8(5)		

Table S5. Selected bond lengths (Å) and angles (º) for compound **11**.

Sm(1)-N(1)	2.525(10	Cr(1)-C(4)	2.069(13)
Sm(1)-N(2)	2.509(10)	Cr(2)-C(2)	2.071(12)
Sm(1)-N(7)	2.555(10)	C(1)-N(1)	1.153(15)
Sm(1)-N(8)	2.580(9)	C(2)-N(2)	1.154(14)
Cr(1)-C(1)	2.082(13)	C(3)-N(3)	1.166(18)
Cr(1)-C(3)	2.051(15)	C(4)-N(4)	1.138(17)
N1-Sm1-N2	146.3(3)	N2-C2-Cr2	177.0(10)
N1-Sm1-O1	75.6(3)	C1-Cr1-C3	91.2(5)
N1-Sm1-O2	79.2(3)	C1-Cr1-C4	88.6(5)
C1-N1-Sm1	164.9(9)	C3-Cr1-C4	90.1(5)
C2-N2-Sm1	163.9(8)	O1-Sm1-O2	84.0(3)
N1-C1-Cr1	175.6(10)		